Available online at www.sciencedirect.com

jmr&t Journal of Materials Research and Technology

www.jmrt.com.br

Original Article

Effect of ohmic-drop on electrochemical performance of EDLC fabricated from PVA:dextran:NH_4I based polymer blend electrolytes

Shujahadeen B. Aziz[a,b,*], *M.A. Brza*[a,c], *M.H. Hamsan*[d], *M.F.Z. Kadir*[e], *S.K. Muzakir*[f], *Rebar T. Abdulwahid*[a,g]

[a] *Advanced Polymeric Materials Research Lab., Department of Physics, College of Science, University of Sulaimani, Kurdistan Regional Government, Qlyasan Street, Sulaimani, Iraq*

[b] *Komar Research Center (KRC), Komar University of Science and Technology, Kurdistan Regional Government, Sulaimani 46001, Iraq*

[c] *Department of Manufacturing and Materials Engineering, Faculty of Engineering, International Islamic University of Malaysia, Kuala Lumpur, Gombak, Malaysia*

[d] *Institute of Post Graduate Study, University of Malaya, 50603 Kuala Lumpur, Malaysia*

[e] *Centre for Foundation Studies in Science, University of Malaya, 50603 Kuala Lumpur, Malaysia*

[f] *Material Technology Program, Faculty of Industrial Sciences & Technology, Universiti Malaysia Pahang, LebuhrayaTunRazak, 43600 Gambang, Kuantan, Pahang, Malaysia*

[g] *Department of Physics, College of Education, University of Sulaimani, Kurdistan Regional Government, Old Campus, Sulaimani, Iraq*

ARTICLE INFO

Article history:
Received 10 November 2019
Accepted 31 January 2020
Available online 10 February 2020

Keywords:
PVA:dextran polymer blend
FTIR study
FESEM
Impedance analysis
TNM and LSV study
EDLC characteristics

ABSTRACT

Proton conducting solid polymer blend electrolytes based on poly(vinyl alcohol)(PVA):dextran that were doped with different quantities of ammonium iodide (NH_4I) were prepared. The X-ray diffraction (XRD) and Fourier-transform infrared (FTIR) study were carried out to examine the compatibility of NH_4I withPVA:dextran polymers. FTIR spectroscopy assessment was used to establish the presence of a complex formation between the PVA:dextran and added salt through the modification and reduction in the intensity of FTIR bands relevant to the functional groups. The field emission scanning electron microscopy (FESEM) examination was used to assess the channels for proton transport. Electrical impedance spectroscopy (EIS) was used to analyse the samples conductivity behaviour. The sample with 20 wt.% of added salt has shown a high DC conductivity which can be employed in electrochemical devices such as EDLC. It is also demonstrated by the transference number (TNM) and linear sweep voltammetry (LSV) that it is appropriate to use the largest conducting sample for electrochemical device. There was electrochemical stability of the electrolyte sample with voltage sweeping linearly to 1.3 V. It is shown by the outcome of cyclic voltammetry (CV) plot that charge storage at the site of

* *Corresponding author at*: Advanced Polymeric Materials Research Lab., Department of Physics, College of Science, University of Sulaimani, Kurdistan Regional Government, Qlyasan Street, Sulaimani, Iraq.
E-mails: shujaadeen78@yahoo.com, shujahadeen.aziz@univsul.edu.iq (S.B. Aziz).

https://doi.org/10.1016/j.jmrt.2020.01.110

electrode-electrolyte is non-Faradiac. A high drop voltage ($V_d = IR$) is implied by the usual galvanostatic charge-discharge. The equivalent series resistance (R_{es}) increases as a result of the increase in V_d all the way through the charge-discharge cycle. Specific capacitance (C_{sp}) is nearly constant from the foremost cycle to the 100th cycle, with average of 4.2 F/g.

1. Introduction

The interdisciplinary field that is extremely specialized is representative of polymer electrolytes, including the domains of polymer science, electrochemistry, organic and inorganic chemistry. The electrolyte systems have a wide range of applications and they have been studied broadly by researchers in both fundamental and industrial domains [1,2]. Recognition has been awarded to the investigations and development of solid polymer electrolytes (SPEs), signifying a substitute for the conventional organic sol–gel electrolytes in the forthcoming years. SPEs own many crucial properties such as dimensional durability, convenient processability, comparatively extensive potential window, flexibility and to a significant degree safety [3]. A lot of attentions were given for examining SPEs as novel materials that have unique properties in the 1970s. It should be asserted that this field was led by Wright and his colleagues, with their study focusing on mixtures of ionic conducting polymer-salt. This is followed by the study of Armand and his colleagues that concentrated on polymer-salt complexes [4,5]. Currently, researchers paid big attention to the electrolytes in the development of thin films for specific objectives that will be subsequently elaborated upon. Nonetheless, the most significant issue that is faced pertains to environmental waste, for example non-biodegradability of petrochemical-based plastic packaging films, and it is because of this that researchers have shown interest in using renewable natural biopolymer-based films. In addition, the two advantages of these electrolytes are non-toxicity and edibility. Furthermore, in many of these films, oxygen and carbon dioxide barrier properties are created because of tightly packed, hydrogen-bonded network structure, and these have been considered as potential electrolytes [5,6]. For instance, a material that is selected for its comparatively large dielectric strength, acceptable charge storage capacity, is poly (vinyl alcohol) (PVA). The electrical and optical properties of PVA are dependent on the dopant's identity. In its structure carbon chain backbone included with hydroxyl groups that are connected to methane carbons. The hydrogen bonding ability derives from these OH groups, which then supports the creation of polymer blends [7]. In addition, the key attributes of PVA are polarity, chemical resistance, satisfied thermo-stability, convenient processability and transparency [8]. In the environmental context, PVA is a water-soluble, non-toxic, extremely crystalline, biocompatible, and biodegradable polymer. Furthermore, its chemical and physical qualities are desirable, having an excellent film-forming ability [9].

Various techniques have been used to enhance the conductivity of polymer electrolytes that have been explained adequately in previous studies. Insertion of nano-fillers, plasticizer and polymer blending are among the common approaches used to improve the conductivity [10,11]. Out of these, polymer blending can be processed and moulded with least efforts, while also exhibiting comparatively higher flexibility. Moreover, there are several uses of this approach, such as combining various polymer matrixes in the contemporary electronic industry [12,13]. Blending has been used broadly for PVA polymer with other functional polymers. For instant, biopolymers and various others compounds having polar properties were used in several industrial applications so as to improve the mechanical property, and making it consistent with dopant species [14].

Dextran polymer is released by surplus sucrose solution after being converted to dextran [15]. The structure of dextran is such that its 1,6-α-D-glucopyranosidic bond can be broken easily, which indicates that it is biodegradable and a non-toxic polymer [16]. It can be initially seen that there are two key functional groups in the backbone of dextran, like hydroxyl and glycoside bond that contain electron lone pairs which carry out the ionic conduction [17,18]. Researchers are able to use the blending technique of two or more polymers to improve the characteristics of individual polymers. Polymer electrolytes are often used in energy devices, such as electrochemical double-layer capacitors (EDLCs), serving as possible substitutes for the traditional lithium batteries. Long lifecycle, safety, fabrication cost effectiveness and excellent performance are among the highly desired properties of EDLC [19,20].

Activated carbon is the most widely known active material that is employed during the creation of EDLC electrode. However, it is important to bring additional enhancements to this carbon material so that the activated carbon electrodes are well compatible with polymer electrolytes [21,22]. Activated carbon is superior because of its distinct properties, i.e. comparatively high electronic conductivity, low cost and acceptable chemical stability [23].

Activated carbon is known for its relatively higher surface area of activated carbon. As a result, high double layer created among the ions from the electrolyte and electrode surface. This is an important quality for energy devices, particularly EDLCs that can preserve greater amounts of energy. Charge storing in EDLCs can be carried out through a non-Faradaic process. This can be explained further by stating that ions from the electrolyte perform charge compensation to the electrons from the electrodes by shifting in the direction of the electrode surface [24,25].On the other hand, EDLCs exhibit superiority in comparison to the Faradaic capacitor or pseudocapacitor with respect to comparatively greater stability, power density, thermal stability, larger reversibility, safety, cost-effectiveness and simpler fabricated techniques [26–28].

Hence, the purpose of the current study is to determine if PVA:dextran based polymer electrolyte is appropriate for EDLC applications.

2. Experimental method

2.1. Preparation of polymer blend electrolytes

This study uses polyvinyl alcohol (PVA) and dextran powder (average molecular weight 35,000–45,000) obtained from Sigma-Aldrich in the form of raw materials to create polymer blend films through the solution cast technique. In this technique, 40 mL of distilled water was used to dissolve 1gm of PVA at a temperature of 80 °C. Once the solution had reached room temperature, it was combined with 40 wt.% of dextran. A homogenous solutions were obtained by stirring the solutions for 2 h with a magnetic stirrer. The terms PVDX0, PVDX10, and PVDX20 were used to code the samples for PVA:dextran combined with 0, 10, and 20 wt.% of ammonium iodide (NH_4I) salt, respectively. After this, the mixtures were cast in distinct clean and dry plastic Petri dishes, which were kept at room temperature to dry till the solvent free films were attained. The films were placed in desiccators with blue silica gel desiccant to achieve additional drying.

2.2. Impedance measurement

Electrical impedance spectroscopy (EIS) spectra of films were achieved by carrying out the EIS measurements with the help of the HIOKI 3531 Z LCR Hi-tester at the ambient temperature, with the frequency ranging from 50 to 1000 kHz. There was hyphenation of the LCR meter to computer-based data collection software, where the real and imaginary parts of the impedance may appear. The polymer blend films were cut into discs with 2 cm diameter. The discs were placed in the middle of two similar circular stainless steel electrodes experiencing spring pressure to make sure that there was a good contact.

2.3. Transference number (TNM) and linear sweep voltammetry (LSV) measurements

V&A instrument DP3003 digital DC power supply was used to examine the ionic (t_i) and electronic (t_e) transference number. The largest conducting polymer electrolyte was located in a Teflon holder with alike stainless steel electrodes. A voltage of 0.80 V was applied to the cell at ambient temperature. The equations given below was used to identify t_i and t_e [29]:

$$t_i = \frac{I_i - I_{ss}}{I_i} \quad (1)$$

$$t_i = 1 - t_e \quad (2)$$

where I_{ss} denotes the saturation current (electronic current lone) and I_i denotes the initial current.

The linear sweep voltammetry (LSV) was employed via Digi-IVY DY2300 potentiostat to examine the electrolyte electrochemical stability. The electrolyte was located in the middle of two stainless steel of a Teflon holder with a scan rate of 50 mV s^{-1}.

2.4. EDLC preparation

Activated carbon of 3.25 g was mixed with 0.25 g of carbon black with planetary ball miller before adding the mixture to 15 mL solution of *N*-methlypyrrolidone as well as 0.50 g of polyvinylidene fluoride (PVDF). After dissolution, a thick and black solution were obtained. After cleaning the aluminium foil with acetone, it was compressed over a glass surface. The solution was streamed and coated on the foil using the doctor blade. Oven was used to dry the electrodes at a temperature of 60 °C. The dried electrodes were reserved in a desiccator for carrying out further drying. The electrode was disintegrated into a small circle shape that spanned an area of 2.01 cm^2. The polymer electrolyte with the highest conductivity was located in the middle of two activated carbon electrodes and held within a coin cell of CR2032. The properties of the fabricated EDLC were studied by Cyclic voltammetry (CV) at 100 mV s^{-1}. Neware battery cycler was used to determine the EDLC charge and discharge profiles with the current density being 0.2 mA cm^{-2}. The following equation can be used to determine the specific capacitance (C_{sp}) of the EDLC:

$$C_{sp} = \frac{i}{xm} \quad (3)$$

where i represents the operating current, x denotes the discharge curve gradient and m represents the mass of the active material. Additional EDLC parameters such as equivalent series resistance (R_{es}), energy density (E_d), as well as power density (P_d) can be demonstrated as [30]:

$$R_{es} = \frac{V_d}{i} \quad (4)$$

$$E_d = \frac{C_{sp}V}{2} \quad (5)$$

$$P_d = \frac{V^2}{4mR_{es}} \quad (6)$$

where V_d represents the drop voltage prior discharging process and V denotes the applied voltage.

3. Results and discussion

3.1. FTIR study

Fourier-transform infrared (FTIR) spectroscopy is a robust method that is used to identify the degree to which atoms and ions interact in polymers or electrolyte systems. The proof of this interaction is obtained by viewing these modifications in the vibrational models inside the polymer electrolyte [31]. The FTIR spectra of PVA:dextran:NH_4I system is demonstrated in Fig. 1. Previous study revealed that any changes in the FTIR band such as fluctuation and increase or decline is a good evidence of existing interactions among polymers or polymer and salts [32]. C–H rocking is believed to bring about absorption peaks at 836 cm^{-1} and 831 cm^{-1} [31]. Absorption peaks at 1415 cm^{-1} and 1420 cm^{-1} have been found to be consistent with $-CH_2$ wagging [33]. A wide and powerful absorption peak was observed at 3314 cm^{-1} and 3332 cm^{-1}, which may

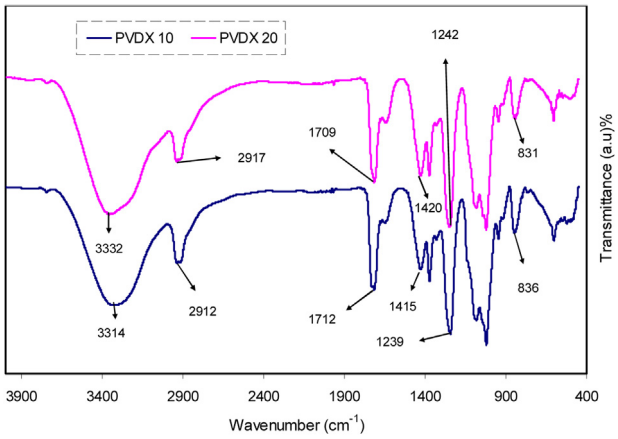

Fig. 1 – FTIR spectra of (i) PVDX10 and (ii) PVDX20 in the region 400 cm^{-1} to 4000 cm^{-1}.

be ascribed to O—H stretching vibration mode [34]. The emergence of high intensity band is another interesting finding, which may be caused by the presence of powerful hydrogen bonding of intra and inter types [20]. Adding 20 wt.% of NH_4I to the sample resulted in shifting in the position with intensity reduction of this band. There is a comparatively weaker peak at 1634 cm^{-1}, which is assigned to C=O stretching of acetate group as a residual part of PVA [33]. At 2917 cm^{-1}, the C–H asymmetric band related to stretching vibration emerged [34]. When the salt concentration was increased, there was an evident shift in the position, with a lower intensity of the band. A typical stretching vibration of the peak at 1076 cm^{-1} is shown in Fig. 1, related to –C–O– in PVA [35].

3.2. *XRD analysis*

PVA:dextran blend and PVA:dextran:NH_4Isystems were exhibited to XRD at ambient temperature. The PVA possesses two peaks at the 2θ values of 20° and 40° [33,35], where dextran possesses two broad peaks at 2θ values of 18° and 23° [18], as documented in earlier reports. In the present work, the peaks of PVA became broader and lower in intensity in the XRD pattern of the PVA:dextran blend film (Fig. 2(a)). It is remarkable that, as designated by the peaks, the PVA:dextran film is not as crystalline as pure PVA as well as its structure is closely amorphous.

Meanwhile, this investigation has perceived that, when NH_4I salt was added, the PVA:dextran blend peaks subjected intensity decline and its wide nature was improved as portrayed in Fig. 2(b,c). Such remarks endorse the amorphous nature of the electrolytes, which enhances larger conductivity by enhancing diffusivity of ions. Additionally, the absence of any peaks related to pure NH_4I confirms the complete dissociation of NH_4I salt in the polymer blend electrolyte. The removal of hydrogen bonding among the chains of polymers is a possible cause for the widening at 20 wt.% NH_4I salt and the decline in intensity, indicating the dominance of the amorphous nature in the system [31]. Furthermore, the polymer blends electrolyte shows little crystalline peaks.

3.3. *Morphology appearance*

Surface morphology is managed by using field emission scanning electron microscope (FESEM). Fig. 3(a–c) demonstrates the FESEM of pure PVA:dextran and blend electrolytes. The surface structure of the SPE samples can be seen from the captured images which can be used to analyse and study the behaviour of the prepared samples [36]. For proton conducting SPEs, a more extensive analysis clearly demonstrates all channels for moving proton over film surface (refer to Fig. 3(b,c)) [37]. There is an increase in the number of white specs when ammonium iodide salt increases from 10 to 20 wt.% as shown in Fig. 3(b,c). These ions in the polymer blend host are considered to be responsible for the conduction process [11]. The impedance analysis of the samples would be carried out in the subsequent section to offer further information on these phenomena.

3.4. *Impedance study*

Electrochemical impedance spectroscopy (EIS) can be used successfully to determine the electrochemical characteristics and ion passage behaviour of electrodes as well as polymer electrolytes of ion-conducting materials [38,39]. For all samples, the EIS spectra including ($Z_{imainary}$ vs Z_{real}) were obtained. Fig. 4(a–c) demonstrates the impedance of pure PVA:dextran and polymer blend electrolytes. It can be noted that at high and low frequency areas there is a single semicircle and a tail separately for the PVA:dextran:NH_4I system as presented in Fig. 4(b,c). A spike emerged at low-frequency region, which may be related to the creation of electric double layer (EDL) capacitance because of charge build-up over the electrode-electrolyte interfacial region [40]. The data point inclination at the short frequency area have to be 90°, however this inclination is provided due to the double-layer capacitance at the electrodes [41]. The extent of claim of SPEs depends on the conductivity in particular, irrespective of the ionic conductions species [42]. Material resistance at the bulk (R_b) can be attained by using the intercept of the semicircle with the real axis (Z_r) at low frequency (end) [43]. Furthermore, the semicircle at the high-frequency is identical to the resistance at the bulk (R_b) and the capacitance at the bulk in parallel connection for the SPEs [44–46]. These points in which the semicircle intersects with the real axis (Z_r) are used to ascertain the R_b value. To determine the film conductivity, two parameters have been considered, which are the value of R_b and the sample dimensions. In this regard, the equation given below can be used:

$$\sigma_{dc} = \left(\frac{1}{R_b}\right) \times \left(\frac{t}{A}\right) \quad (7)$$

Here t signifies the polymer electrolyte film thickness and A refers to the film surface area. The distinct spike region at 20 wt.% NH_4I is a good evident to show that ion diffusion is the sole method that is used for ion transport [47]. This ion diffusion dominancy can be confirmed by looking at the highest conductivity of 2×10^{-5} S/cm which was obtained for PVA:dextran doped using 20 wt.% NH_4I at ambient temperature. In addition, it was noted that DC ionic conductivity of PVA:dextran improved considerably when distinct concentrations of NH_4I were added, as presented in Table 1. It is believed

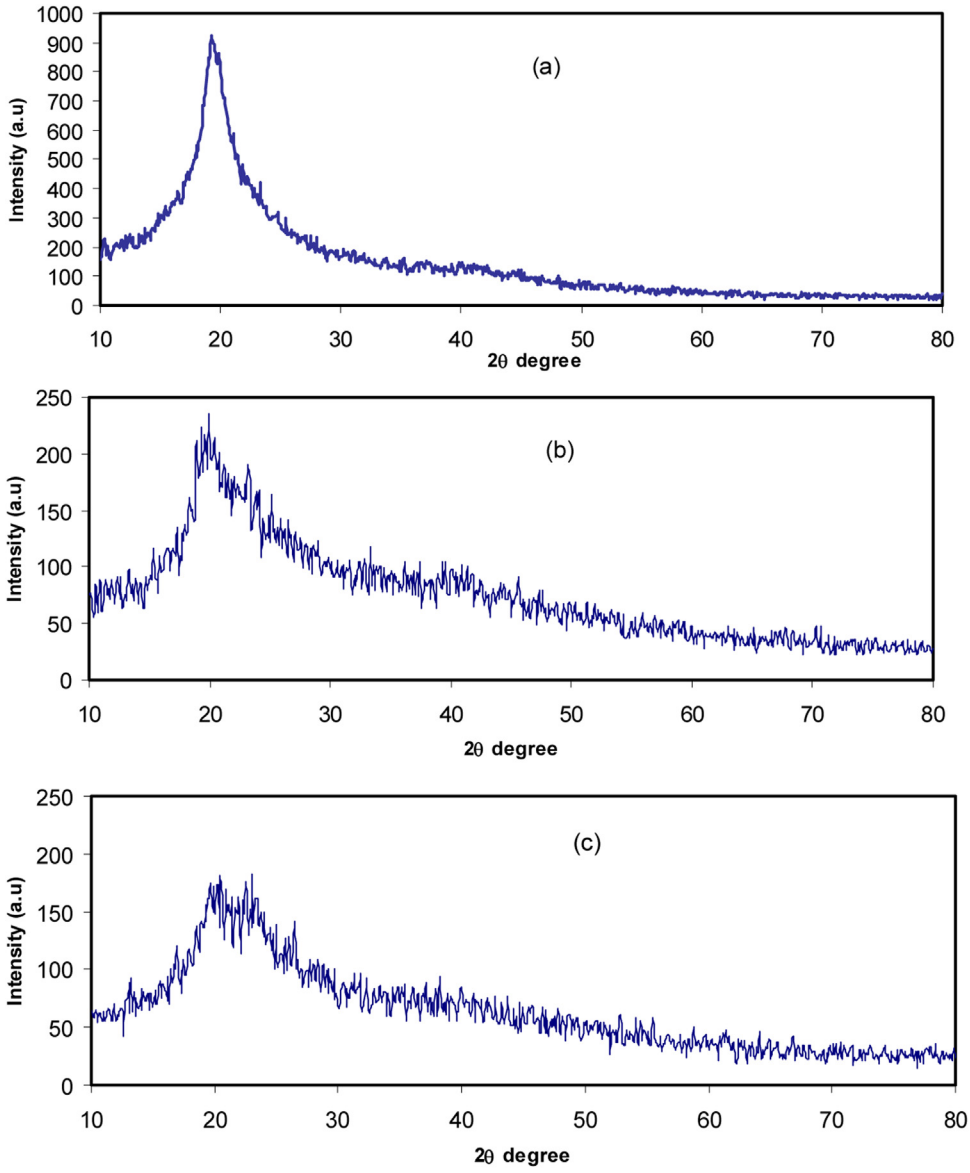

Fig. 2 – XRD pattern for (a) pure PVA:dextran, (b) PVDX10 and (c) PVDX20 films.

Table 1 – Calculated DC conductivity for neat PVA:dextran and blend electrolyte films at room temperature.

Sample designation	DC conductivity (s cm^{-1})
PVDX 0	9.55×10^{-9}
PVDX 10	2.27×10^{-8}
PVDX 20	2.08×10^{-5}

that an increase in ion mobility as well as charge carrier concentration improve the DC conductivity, which is depicted mathematically at ambient temperature as follows [48,49]:

$$\sigma = \sum_{i} n_i q_i \mu_i \quad (8)$$

Here n_i, signifies the charge carrier density, q_i refers to the typical meaning (1.6×10^{-19} C), and μ_i signifies the ion mobility. There was an increase in ionic conductivity (σ) when charge carrier concentration and ionic mobility within the system increased, asit is evident from Eq. (8). The data shown in both Table 1 and impedance spectra clearly shows that when ammonium iodide salt concentration increased, there was an increase in DC conductivity.

3.5. *EDLC characteristics*

3.5.1. *Transference number (TNM)*

TNM is used to validate the main charge carrier within the polymer electrolyte. After applying the 0.80 V, the current begins to drop until it reaches the saturation region. The polarization of current as a function of time for the highest conducting electrolyte is depicted in Fig. 5. The reason for the high value of the initial current is because of the part played by the electron as well as the ion at the initial stage. Fig. 5 shows that there was a significant decrease in the current before it

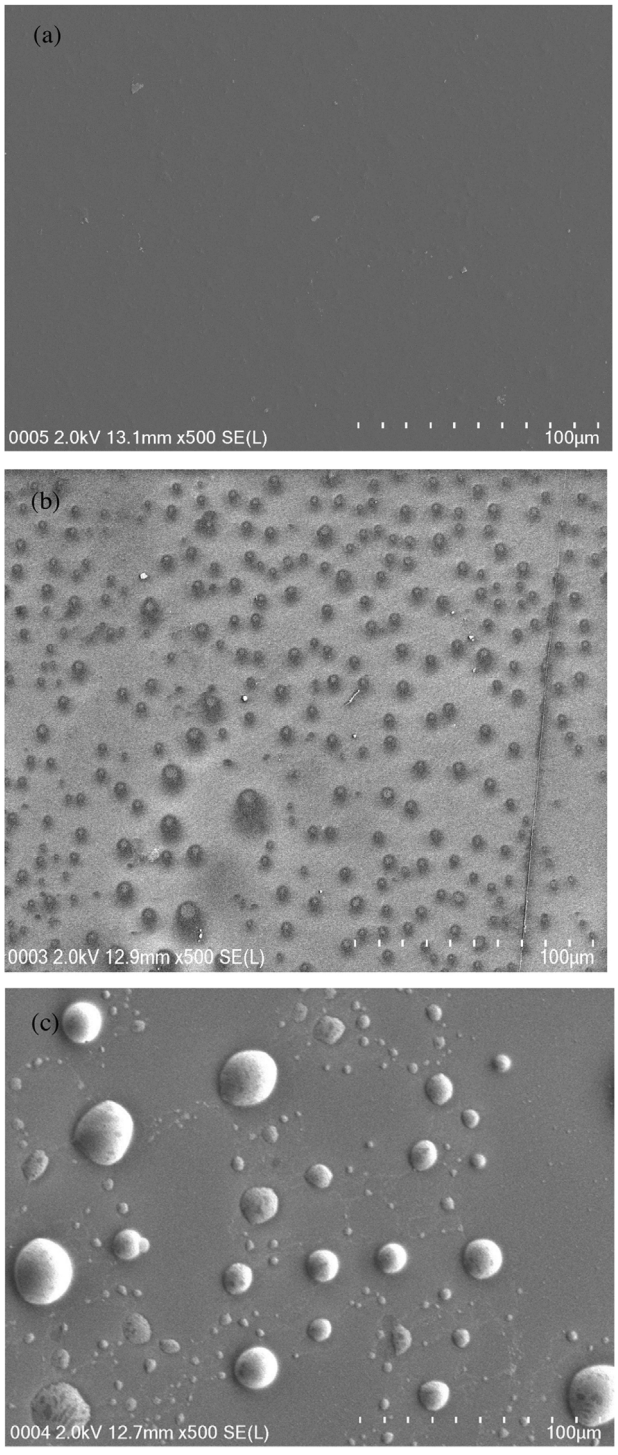

Fig. 3 – Field emission scanning electron microscopy (FESEM) images for (a) PVDX0, (b PVDX10, and (c) PVDX20 blend electrolytes.

attained a steady state. The cell is polarized when it is in the steady state, while the rest of the current flow is because of electron. The reason for this is the ionic blocking impact by stainless steel electrodes, which allows just the electron to move through [50]. Eqs. (1) and (2) are used to compute t_i and t_e values, while achieving the values of I_i and I_{ss} as 10.5 µA and 0.19 µA, respectively. The values of t_i and t_e are found to be 0.981 and 0.019, respectively. The t_i value is of great interest as it is in close proximity of the ideal value of 1. Consequently, it is concluded that ions play the key role in the migration process in the thePVA:dextran:NH_4I system.

This finding is similar to the system of glycerolized potato starch-methyl cellulose (MC)-ammonium nitrate (NH_4NO_3)-based electrolyte that was presented by Hamsan et al. [29]. It was determined by Wang et al. [51] that PVA-LiTFSI-EMITFSI has ionic transference number of 0.995.

3.5.2. *Electrochemical stability determination*

It is only on the highest conducting PVA:dextran:NH_4I system subjected electrochemical stability determination by performing linear sweep voltammetry (LSV) analysis. Study the electrochemical stability window is considered as a curial property of the used material in any electrochemical devices including capacitor and proton battery [52]. The performance of a device can be tested when one is aware of the electrochemical stability of the sample before the charge-discharge cycling test. To avoid causing any damage to the electrolyte, the breakdown voltage is critical. In the current work from the LSV analysis it was found that the electrochemical stability window of the largest conducting system was almost 1.3 V. The maximum applied voltage in this study reached 0.80 V; hence, there should be electrochemical stability of the electrolytes to be used in the EDLCs. Fig. 6 shows the LSV plot of the highest conducting sample. A scan rate of 50 mV s^{-1} is used to sweep the voltage from 0 V to 4 V, till a high current is noticed at a given potential. No evident current is seen through the electrode potential from 0 V to 1.3 V. When the electrode potential reached above 1.3 V, a drastic increase in the value of the current observed which is linked to the decomposition of SPE at the inert electrode interface [53]. According to Pratap et al. [54], the typical electrochemical window for proton batteries is approximately 1 V; hence, in the current study, there is a sufficient breakdown voltage to ensure that PVA:dextran:NH_4I blend polymer electrolyte works safely within any protonic device.

This result is comparable to that obtained by other ammonium salt based polymer electrolytes. A plasticized system of methyl cellulose (MC) incorporated with ammonium bromide (NH_4Br) exhibited the electrochemical stability of 1.53 V was presented by Kadir et al. [21]. This did not show an evident current passing within the working electrode from open circuit potential to the decomposition voltage. When the electrode potential was more than the decomposition voltage, there was an increase in the current gradually. The study by Woo et al. [55] showed that the electrochemical stability of poly(ε-caprolactone) (PCL)-based polymer electrolytes (PE)-ammoniumthiocyanate (NH_4SCN) is almost 1.4 V, and it was used in the production of EDLC. Therefore, based on the results presented here it can be concluded that the largest conductingPVA:dextran:NH_4I system is electrochemically stable to be used in electrochemical devices.

3.5.3. *Cyclic voltammetrytest for the EDLC*

Cyclic voltammetry (CV) examinations of the EDLCs can be used to determine the type of charge storage carried out at the electrode-electrolyte interfaces [56]. The CV of the assem-

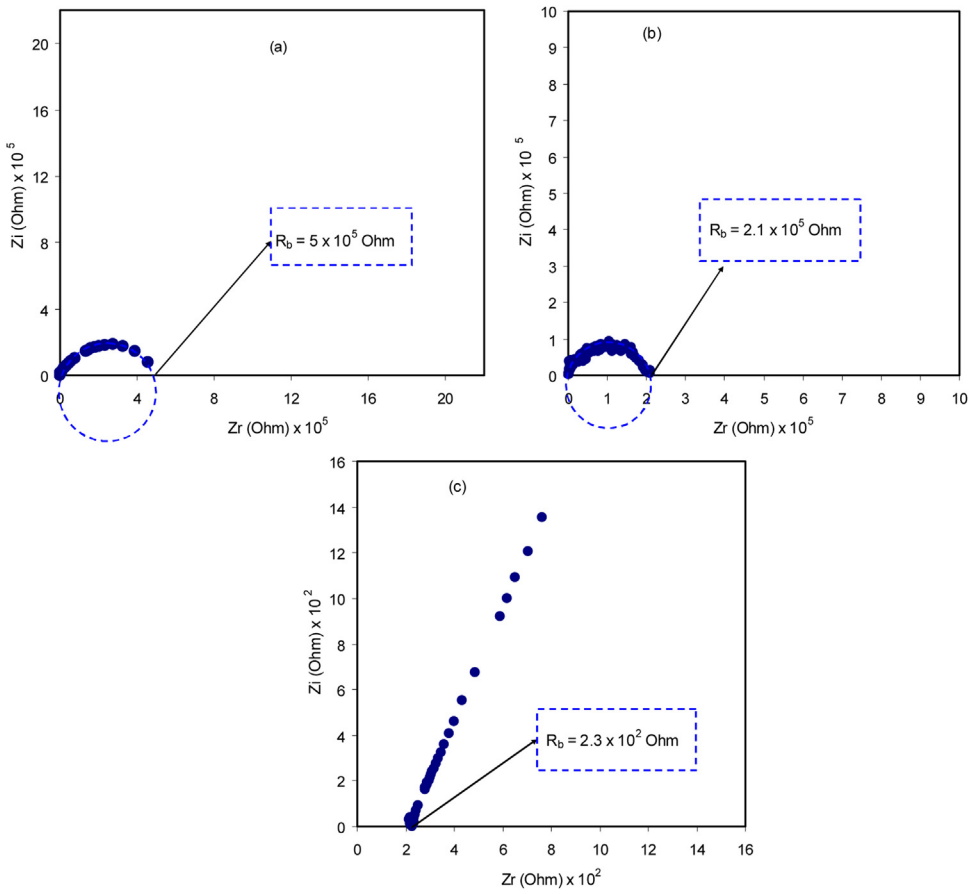

Fig. 4 – Experimental Impedance plots for (a) PVDX0, (b) PVDX10, and (c) PVDX20 blend electrolyte films.

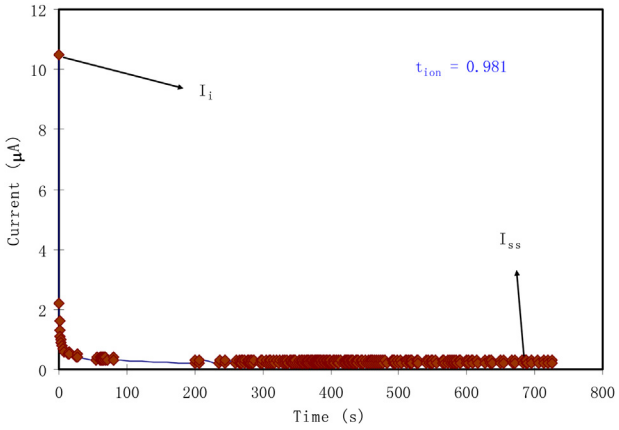

Fig. 5 – Polarization current versus time for the highest conducting (PVDX20) electrolyte film.

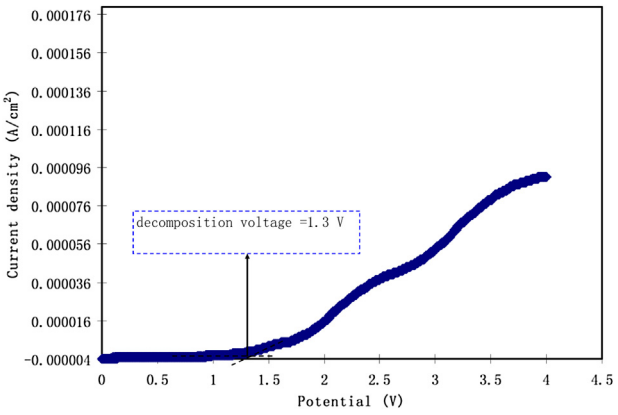

Fig. 6 – Linear sweep voltammetry (LSV) plot for the highest conducting (PVDX20) blend electrolyte film.

bled cell at scan rate of 100 mV/s at room temperature is demonstrated in Fig. 7. The peak absence in the plot verify that there was no redox reaction in the potential range of 0–1 V. It is shown by this phenomenon that electrical double layer capacitors are present [57]. A lack of redox peak confirms the insignificant part played by electrons, suggesting that non-faradic process takes place in the creation of supercapacitor, which endorses its EDLCs behavior [58]. The basis of the charge storage mechanism in EDLC is the collection of ions at the electrode-electrolyte interfaces when an electric potential is applied [59]. There is a small diversion from the rectangular shape of CV in Fig. 7 in contrast to those obtained in previous studies that resembled a leaf-like shape [55,59]. The voltammograms shape obtained in this study is similar to that presented by Hamsan et al. [29]. In their work the cyclic voltammograms at the scan rate of 20 mV/s for EDLCs

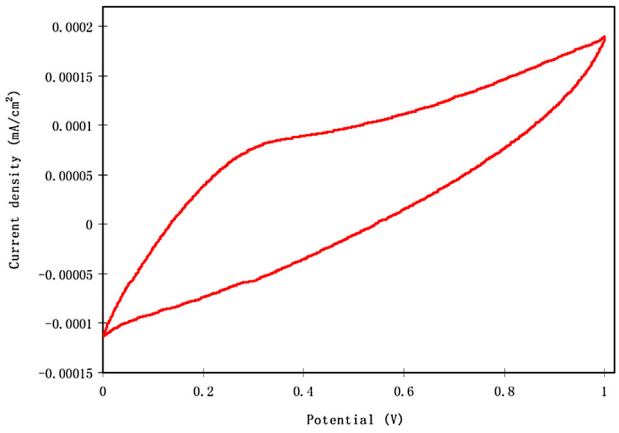

Fig. 7 – Cyclic voltammetry (CV) plot of the fabricated electrical double layer capacitor (EDLC) from PVDX20 film in the potential range of 0 V to 1 V.

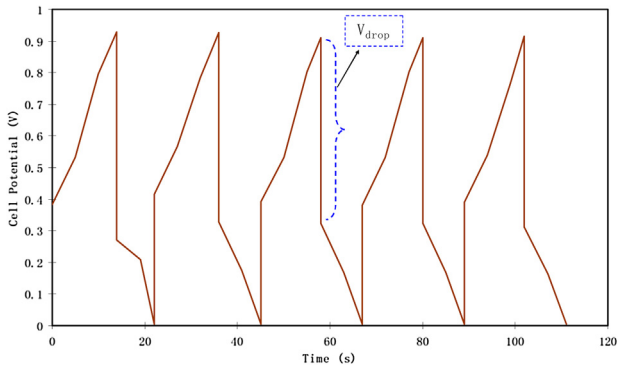

Fig. 8 – Charge–discharge profiles for the fabricated EDLC at 0.5 mA cm^{-2}.

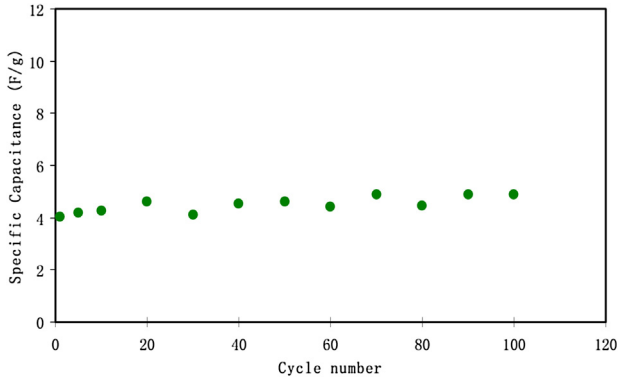

Fig. 9 – Specific capacitance of the fabricated EDLC for 100 cycles.

were created with the system of glycerolized potato starch-MC-NH_4NO_3-based polymer electrolyte [29].

An ideal EDLC exhibits a perfect rectangular shape of CV. Because of the high scan rate, the cyclic voltammogram shape deviates from an ideal rectangular shape due to the carbon porosity, which causes a current dependence on voltage [60]. In addition, the previous studies have shown that there is discrepancy from the rectangular shape because of various reasons. According to Pandey et al., the discrepancy is because of the rapid build-up of the electric double layer [61]. The deviation from the rectangular shape is may also be caused by the equivalent series resistance (R_{es}) of the EDLC. This consistof the resistance between the electrode and the current collector, the resistance at the interface between the electrode and the electrolyte, the electrode intrinsic resistance, and the resistance of the electrolyte at the bulk [62].

A sudden drop in voltage (V_d) when the EDLC is discharging is known as internal resistance (refer to charge-discharge curve) [59,60]. There is a decline in V_d at the beginning, which subsequently rises when charge-discharge cycles increase, bringing about a conflicting differentiation in specific capacitance. Nonetheless, it can be observed that in the current study, C_{sp} is almost constant during 100 cycles, which suggests that it has perfect cyclic stability. A significant standard for appropriate performance is the long cycle lifetime of EDLC. Furthermore, in this study two other essential parameters which are energy and power densities, are also discussed in the subsequent section which confirms that there is actual usage of an EDLC device.

3.5.4. *EDLC characterization*

Fig. 8 demonstrates the standard galvano static charge–discharge features of the fabricated EDLC. There is additional proof on the presence of charge double-layer or capacitive features when there is nearly linear gradient of the discharge parts [63]. The slope value of the discharge curves is substituted in Eq. (3) to obtain the value of C_{sp}. The C_{sp} values of the EDLC up to 100 cycles at scan rate of 50 mV/s is demonstrated in Fig. 9. At the high scan rates, energy loss rises and the stored charge on the surface of the electrode declines and causes a reduction in C_{sp} value [64]. It is manifest that C_{sp} is nearly constant from 1st cycle up to 100th cycle with average of 4.2 F/g. Despite the fact that in other studies enormous lessening of C_{sp} was perceived at great number of cycles. They considered that the lessening of these electrochemical properties might be the development of ion agglomeration. The mobile ions desire to be coupled or agglomerated after the quickprocesses of charge and discharge. The ionic movement in the electrolyte can be restricted by these ion pairs which in turn reduce the ion adsorption into the carbon pores. This diminishes the creation of adsorbed ions at the interface of electrode and electrolyte. Consequently, the specific capacitance, energy density, as well as power density of EDLC decline with rising the number of cycles [65].

The values of the capacitance achieved in the current work are higher than that in the earlier literature. Liew et al. [65] documented that the specific capacitance of EDLC cell with PVA-ammonium acetate (CH_3COONH_4) exhibits specific capacitance of 0.13 F/g within 500 cycles. As documented by Shuhaimi et al. [66], un-plasticized methyl cellulose (MC)-based electrolyte (MC-Ammonium nitrate (NH_4NO_3)) when utilized in a capacitor produces small capacity of approximately 1–2 F/g. It was determined by Feng et al. [22] that carboxymethyl cellulose (CMC)-NH_4NO_3-based solid polymer electrolyte has specific capacitance of 1.8 F/g.

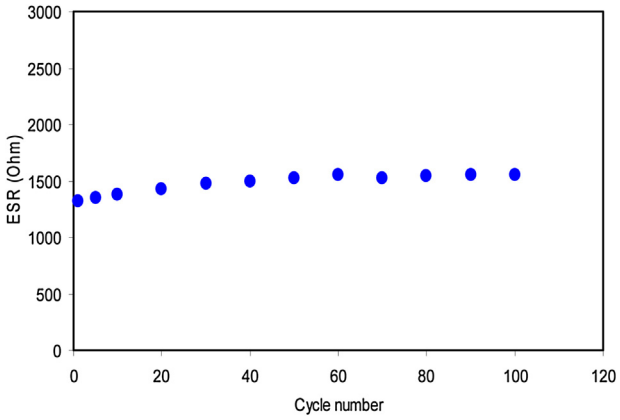

Fig. 10 – The pattern of equivalent series resistance of the EDLC for 100 cycles.

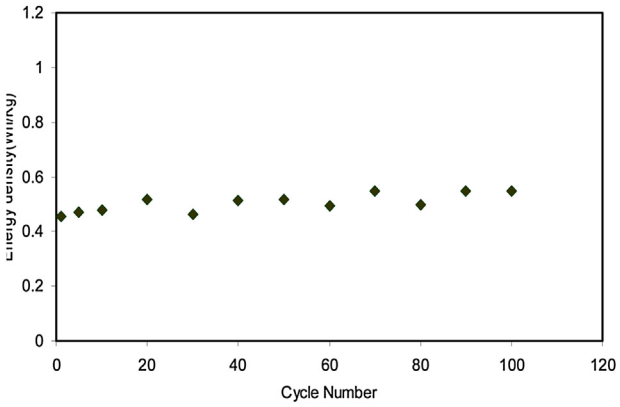

Fig. 11 – Energy density of the fabricated EDLC for 100 cycles.

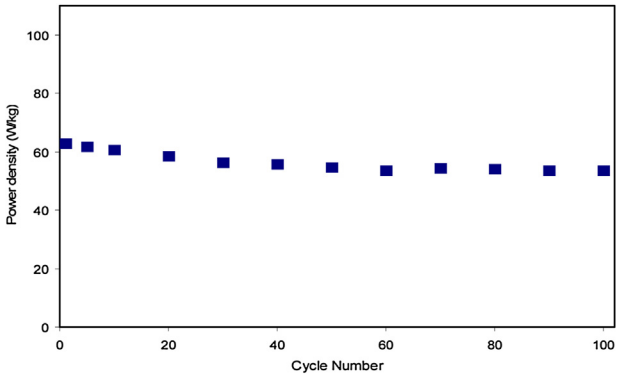

Fig. 12 – Power density of the fabricated EDLC for 100 cycles.

The value of C_{sp} in the current work is comparable with other studiesusing different SPEs. Other investigators documented for instance 4 F/g and 4.3 F/g for PEO_9/lithium trifluoromethane sulfonate ($LiCF_3SO_3$) plasticized with 50 wt.% poly(ethylene glycol) (PEG)200, as well as polyvinylidene fluoride-hexafluoropropylene (PVDF-HFP)(25%) + PC_{10}-EC_{10}/lithium perchlorate ($LiClO_4$), correspondingly [67,68]. Compared to our previous work [69,70], the value of C_{spe} is small. This can be attributed to high Ohmic-drop in charge–discharge profile.

As perceived in Fig. 8, there is a potential drop prior the beginning of each discharge process. The internal resistance termed as equivalent series resistance (R_{es}) is responsible for this potential drop which has been determinedfrom Eq. (4). As illustrated in Fig. 10, R_{es} of the EDLC is in the range between 1350 and 1500 Ω. The existenceof R_{es} in the EDLC is primarily attributable to three resistances whichmay be current collector, polymer electrolyte at the bulk, and space between electrode and electrolyte [71]. Kumar and Bhat [72], reported that the rise in voltage reduction within the charge and discharge cycles which causes the intensification in R_{es} is because of the degradation of polymer electrolyte in the EDLC. The R_{es} of the EDLC in the current work is comparable to that (1300 Ω) documented for ionic liquid integrated polyethylene oxide (PEO) based electrolyte [56], while it is higher than those reported for other EDLC based devices [73,74].

The E_d values in the current workcomputed from Eq. (5) can be seen in Fig. 11. At initial cycles the value of E_d has a tendency torise toward the 20th cycle. The value of E_d graduallydeclines and stays nearly constant throughout the cycles beyond the 20th cycle up to 100 cycles with average of 0.55 Wh/kg. consequently, it can be presumed that from 20th cycle up to 100th cycle, the passage of ion possesses nearly the same energy barrier [75]. The diminution in E_d value through the number of cycles is related to the rise in the internal resistance that causes the raise of energy loss throughout the charging–discharging cycles [60,76]. The value of energy density acquired in the present work is higher than the previous literature. Other researchers documented for instance 0.17 Wh/kg and 0.31 Wh/kg for PVA:CH_3COONH_4):BmImTf, as well as PVA: 250 wt% PMI-TFSI, correspondingly [77,78].

The value of P_d calculated from Eq. (6) for this work can be seen in Fig. 12. As appeared in Fig. 10, R_{es} of the EDLC is nearlycomparable pattern with the power density in Fig. 12. At initial cycles the value of R_{es} is witnessed to rise and consistent beyond 20th cycle where the P_d valuedeclines and accomplishedstableafter 20th cycle. Upon charge and discharge for 100 cycles, the EDLC power density exhibits a drop from 64 to 58 W/kg. The outcome of the present work is higher than that accomplished by Zheng et al. [79] who documented the power density of (1.5 Mtriethyl methyl ammonium tetrafluoroborate ($TEMABF_4$)/propylene carbonate (PC)) as about 30 W/kg.

The lower values of P_d are declined as the number of cyclesenlarged. This drop tendency harmonized with the growing tendency of R_{es}. The raise of internal resistance is because of electrolyte depletions and ion agglomeration after the fast charge–discharge processes consequently provides lower power density at large number of cycles [80]. When ions of the polymer electrolyte are migrated into the double layers at the interfaces of the electrode and electrolyte, there is a diminution of the concentration of salt in the polymer electrolyte (termed electrolyte depletion) that limits the capacitor energy density. Therefore, the drop of power density, energy density, and specific capacitance is by reason of the electrolyte depletion. Furthermore, ion combination after the fast charged–discharged processes will block the movement of ions toward the surface of the electrodes that causes ion

adsorption lessening at the interfaces of the electrode and electrolyte [65].

4. Conclusions

To conclude, proton conducting solid polymer blend electrolytes (SPBEs) based on PVA:dextran doped with different amounts of ammonium iodide (NH_4I) are appropriate for use in energy storage EDLC. The structural examination displayed broad and low intensity peaks in the XRD spectra by means of the distraction of hydrogen bonding inside the polymer chains. The NH_4I compatibility as a proton provider within the PVA:dextran was examined through the FTIR study. When the salt concentration was increased, there was an evident shift in the position, with a lower intensity of the band. The channels for proton transference were perceived through the appearance of various white balls with different sizes in the FESEM investigation. The conductivity behavior of the films was examined using EIS. The high DC conductivity of the PVA:dextran blend electrolyte at 20 wt.% of added salt is found to be 2.08×10^{-5} s/cm. The TNM analysis reveals the dominance of ion in the SPBEs. The LSV outcome reveals the stability of the blend SPE sample up to 1.3 V and so it can be say that the sample is convenient for electrochemical device application. The result of CV plot specifies that the type of charge storage mechanism at the interfaces of the electrode and electrolyte is non-Faradiac. A high drop voltage (V_d) is implied by the characteristicgalvanostatic charge–discharge.The equivalent series resistance (R_{es}) increases as a result of the increase in V_d all through the charge–discharge cycle. It is apparent that specific capacitance (C_{sp}) is almost consistent from foremost cycle to 100th cycle with average of 4.2 F/g. The low value of energy density (0.44 Wh/kg) and power density (63 W/kg) can be ascribed to the high value of R_{es} (1357 Ω).

Conflicts of interest

The authors declare no conflicts of interest.

Acknowledgements

The authors gratefully acknowledge the financial support for this study from Ministry of Higher Education and Scientific Research-Kurdish National Research Council (KNRC), Kurdistan Regional Government/Iraq. The financial support from the University of Sulaimani and Komar Research Center (KRC), Komar University of Science and Technology are greatly appreciated.

REFERENCES

[1] Wang YP, Gao XH, Li HK, Li HJ, Liu HG, Guo HX. Effect of active filler addition on the ionic conductivity of PVDF–PEG polymer electrolyte. J Macromol Sci A 2009;46:461–7.
[2] Aziz SB. Li+ ion conduction mechanism in poly(ε-caprolactone)-based polymer electrolyte. Iran Polym J 2013;22:877, http://dx.doi.org/10.1007/s13726-013-0186-7.
[3] Hema M, Selvasekarapandian S, Arunkumar D, Sakunthala A, Nithya H. FTIR, XRD and ac impedance spectroscopic study on PVA based polymer electrolyte doped with NH4X (X = Cl, Br, I). J Non-Cryst Solids 2009;355:84–90.
[4] Fenton DE, Parker JM, Wright PV. Complexes of alkali metal ions with poly(ethylene oxide). Polymer 1973;14:589.
[5] Armand MB, Chabango JM, Duclot MJ. In: Vashishta P, Mundy JN, Shenoy GK, editors. Fast ion transport in solids. 1979. North-Holland, Amsterdam. p. 131.
[6] Salleh NS, Aziz SB, Aspanut Z, Kadir MFZ. Electrical impedance and conduction mechanism analysis of biopolymer electrolytes based on methyl cellulose doped with ammonium iodide. Ionics 2016;22:2157–67.
[7] Mohamed Shaimaa A, Al-Ghamdi AA, Sharma GD, El Mansy MK. Effect of ethylene carbonate as a plasticizer on CuI/PVA nanocomposite: structure, optical and electrical properties. J Adv Res 2014;5:79–86.
[8] Suo Baoting, Su Xin, Wu Ji, Chen Daniel, Wang Andrew, Guo Zhanhu. Poly(vinyl alcohol) thin film filled with CdSe–ZnS quantum dots: fabrication, characterization and optical properties. Mater Chem Phys 2010;119:237–42.
[9] Choo Kaiwen, Ching Yern Chee, Chuah Cheng Hock, Julai Sabariah, Liou Nai-Shang. Preparation and characterization of polyvinyl alcohol-chitosan composite films reinforced with cellulose nanofiber. Materials 2016;9:644, http://dx.doi.org/10.3390/ma9080644.
[10] Aziz Shujahadeen B, Woo Thompson J, Kadir MFZ, Ahmed Hameed M. A conceptual review on polymer electrolytes and ion transport models. J Sci Adv Mater Devices 2018;3:1–17.
[11] Aziz Shujahadeen B, Hamsan MH, Abdullah Ranjdar M, Kadir MFZ. A promising polymer blend electrolytes based on chitosan: methyl cellulose for EDLC application with high specific capacitance and energy density. Molecules 2019;24(13):2503, http://dx.doi.org/10.3390/molecules24132503.
[12] Chen Z, Pei J, Li R. Study of the preparation and dielectric property of PP/SMA/PVDF blend material. Appl Sci 2017;7:389, http://dx.doi.org/10.3390/app7040389.
[13] Aziz Shujahadeen B, Hamsan Muhamad H, Kadir Mohd FZ, Karim Wrya O, Abdullah Ranjdar M. Development of polymer blend electrolyte membranes based on chitosan: dextran with high ion transport properties for EDLC application. Int J Mol Sci 2019;20(13):3369, http://dx.doi.org/10.3390/ijms20133369.
[14] Gaaz Tayser Sumer, Sulong Abu Bakar, Akhtar Majid Niaz, Kadhum Abdul Amir H, Mohamad Abu Bakar, Al-Amiery Ahmed A. Properties and applications of polyvinyl alcohol, halloysite nanotubes and their nanocomposites. Molecules 2015;20:22833–47, http://dx.doi.org/10.3390/molecules201219884.
[15] Sarwat F, Ahmed N, Aman A, Qader SAU. Optimization of growth conditions for the isolation of dextran producing *Leuconostoc* spp. from indigenous food sources Pak. J Pharm Sci 2013;26:793–7.
[16] Barsbay M, Guner A. Miscibility of dextran and poly(ethylene glycol) in solid state: effect of the solvent choice. Carbohydr Polym 2007;69:214–23.
[17] Telegeev G, Kutsevo N, Chumachenko V, Naumenko A, Telegeeva P, Filipchenko S, et al. Dextran-polyacrylamide as matrices for creation of anticancer nanocomposite int. J. Polym. Sci 2017;2017:9. Article ID 4929857.
[18] Hamsan MH, Shukur MF, Aziz SB, Kadir MFZ. Dextran from *Leuconostoc mesenteroides*-doped ammonium salt-based green polymer electrolyte. Bull Mater Sci 2019;42:57, http://dx.doi.org/10.1007/s12034-019-1740-5.
[19] Huo Pengfei, Ni Shoupeng, Hou Pu, Xun Zhiyu, Liu Yang, Gu Jiyou. A crosslinked soybean protein isolate gel polymer

electrolyte based on neutral aqueous electrolyte for a high-energy-density supercapacitor. Polymers 2019;11:863.
[20] Wang Jeng-An, Lu Yi-Ting, Lin Sheng-Chi, Wang Yu-Sheng, Ma Chen-Chi M, Chi-Chang Hu. Designing a novel polymer electrolyte for improving the electrode/electrolyte interface in flexible all-solid-state electrical double-layer capacitors. ACS Appl Mater Interfaces 2018;2018:1021.
[21] Kadir MFZ, Salleh NS, Hamsan MH, Aspanut Z, Majid NA, Shukur MF. Biopolymeric electrolyte based on glycerolized methyl cellulose with NH4Br as proton source and potential application in EDLC. Ionics 2017;24:1651–62.
[22] Feng Y, Chen S, Wang J, Lu B. Carbon foam with microporous structure for high performance symmetric potassium dual-ion capacitor. J Energy Chem 2020;43:129–38.
[23] Wang H, Lin J, Shen ZX. Polyaniline (PANi) based electrode materials for energy storage and conversion. J Sci Adv Mater Devices 2016;1:225–55.
[24] Kiamahalleh MV, Zein SHS. Multiwalled carbon nanotubes based nanocomposites for supercapacitors: a review of electrode materials. Nano 2012;7:1230002.
[25] Shobana V, Parthiban P, Balakrishnan K. Lithium based battery-type cathode material for hybrid supercapacitor. J Chem Pharm Res 2015;7:207–12.
[26] Inagaki M, Konno H, Tanaike O. Carbon materials for electrochemical capacitors. J Power Sources 2010;195:7880–903, http://dx.doi.org/10.1016/j.jpowsour.2010.06.036.
[27] Zhang D, Zhang X, Chen Y, Yu P, Wang C, Ma Y. Enhanced capacitance and rate capability of graphene/polypyrrole composite as electrode material for supercapacitors. J Power Sources 2011;196:5990–6, http://dx.doi.org/10.1016/j.jpowsour.2011.02.090.
[28] Pell WG, Conway BE. Peculiarities and requirements of asymmetric capacitor devices based on combination of capacitor and battery-type electrodes. J Power Sources 2004;136:334–45, http://dx.doi.org/10.1016/j.jpowsour.2004.03.021.
[29] Hamsan MH, Shukur MF, Kadir MFZ. NH_4NO_3 as charge carrier contributor in glycerolized potato starch-methyl cellulose blend-based polymer electrolyte and the application in electrochemical double-layer capacitor. Ionics 2017, http://dx.doi.org/10.1007/s11581-017-2155-1.
[30] Shukur MF, Ithnin R, Kadir MFZ. Electrical characterization of corn starch-LiOAc electrolytes and application in electrochemical double layer capacitor. Electrochim Acta 2014;136:204–16.
[31] Hemaa M, Selvasekerapandian S, Sakunthala A, Arunkumara D, Nithya H. Structural, vibrational and electrical characterization of PVA–NH4Br polymer electrolyte system. Phys B 2008;403:2740–7.
[32] Aziz SB, Hamsan MH, Brza MA, Kadir MFZ, Abdulwahid RT, Ghareeb HO, et al. Fabrication of energy storage EDLC device based on CS: PEO polymer blend electrolytes with high Li^+ ion transference number. Results Phys 2019;15:102584, http://dx.doi.org/10.1016/j.rinp.2019.102584.
[33] Malathi J, Kumaravadivel M, Brahmanandhan GM, Hema M, Baskaran R, Selvasekarapandian S. Structural, thermal and electrical properties of PVA–$LiCF_3SO_3$ polymer electrolyte. J Non Cryst Solids 2010;356:2277–81.
[34] Makled MH, Sheha E, Shanap TS, El-Mansy MK. Electrical conduction and dielectric relaxation in p-type PVA/CuI polymer composite. J Adv Res 2013;4:531–8.
[35] Jiang Long, Yang Tonglu, Peng Leilei, Dan Yi. Acrylamide modified poly(vinyl alcohol): crystalline and enhanced water solubility. RSC Adv 2015;5:86598–605.
[36] Shujahadeen BA, Brza MA, Mohamed PA, Kadir MFZ, Hamsan MH, Abdulwahid RT, et al. Increase of metallic silver nanoparticles in chitosan: AgNt based polymer electrolytes incorporated with alumina filler. Results Phys 2019;13:102326, http://dx.doi.org/10.1016/j.rinp.2019.102326.
[37] Bhad SN, Sangawar VS. Optical study of PVA based gel electrolyte. Int J Sci Eng Res 2013;4:1719.
[38] Cho S, Chen C, Mukherjee PP. Influence of microstructure on impedance response in intercalation electrodes. J Electrochem Soc 2015;162:1202–14, http://dx.doi.org/10.1149/2.0331507jes.
[39] Svensson AM, Valøen LO, Tunold R. Modeling of the impedance response of porous metal hydride electrodes. Electrochim Acta 2005;50:2647–53, http://dx.doi.org/10.1016/j.electacta.2004.11.035.
[40] Aziz SB, Abidin ZHZ, Arof AK. Influence of silver ion reduction on electrical modulus parameters of solid polymer electrolyte based on chitosan-silver triflate electrolyte membrane. Express Polym Lett 2010;4:300–31.
[41] Fonseca CP, Cavalcante F Jr, Amaral FA, Souza CAZ, Neves S. Thermal and conduction properties of a PCL-biodegradable gel polymer electrolyte with $LiClO_4$, LiF_3CSO_3, and $LiBF_4$ salts. Int J Electrochem Sci 2007;2:52–63.
[42] Hamsan MH, Aziz Shujahadeen B, Shukur MF, Kadir MFZ. Protonic cell performance employing electrolytes based on plasticized methylcellulose-potato starch-NH_4NO_3. Ionics 2019;25:559, http://dx.doi.org/10.1007/s11581-018-2827-5.
[43] Pradhan DK, Choudhary RNP, Samantaray BK. Studies of structural, thermal and electrical behavior of polymer nanocomposite electrolytes. Express Polym Lett 2008;2:630–8, http://dx.doi.org/10.3144/expresspolymlett.2008.76.
[44] Pandey Mayank, Joshi Girish M, Deshmukh Kalim, Ahmad Jamil. Impedance spectroscopy and conductivity studies of $CdCl_2$ doped polymer electrolyte. Adv Mater Lett 2015;6:165–71, http://dx.doi.org/10.5185/amlett.2015.5639.
[45] Vanitha D, Bahadur SA, Nallamuthu, Athimoolam Shunmuganarayanan, Manikandan A. Electrical impedance studies on sodium ion conducting composite blend polymer electrolyte. J Inorg Organomet Polym Mater 2017;27:257, http://dx.doi.org/10.1007/s10904-016-0468-6.
[46] Aziz B, Abdullah RM, Kadir MFZ, Ahmed HM. Non suitability of silver ion conducting polymer electrolytes based on chitosan mediated by barium titanate ($BaTiO_3$) for electrochemical device applications. Electrochim Acta 2019;296:494–507.
[47] Baochen W, Li F, Xinsheng P. The impedance study of modified PEO polymer electrolyte. Solid State Ion 1991;48:203–5.
[48] Aziz S, Abdullah R, Rasheed M, Ahmed H. Role of ion dissociation on DC conductivity and silver nanoparticle formation in PVA: AgNt based polymer electrolytes: deep insights to ion transport mechanism. Polymers 2017;9:338, http://dx.doi.org/10.3390/polym9080338.
[49] Aziz SB, Abidin ZHZ. Ion-transport study in nanocomposite solid polymer electrolytes based on chitosan: electrical and dielectric analysis. J Appl Polym Sci 2015;132:41774.
[50] Rani MSA, Ahmad A, Mohamed NS. Influence of nano-sized fumed silica on physicochemical and electrochemical properties of cellulose derivatives-ionic liquid biopolymer electrolytes. Ionics 2017;24:807–14.
[51] Wang Jingwei, Zhao Zejia, Song Shenhua, Ma Qing, Liu Renchen. High performance poly(vinyl alcohol)-based Li-ion conducting gel polymer electrolyte films for electric double-layer capacitors. Polymers 2018;10:1179.
[52] Shuhaimi NEA, Alias NA, Majid SR, Arof AK. Electrical double layer capacitor with proton conducting κ-carrageenan-chitosan electrolytes. Funct Mater Lett 2008;1:195–201.
[53] Tian Khoon L, Ataollahi N, Hassan NH, Ahmad A. Studies of porous solid polymeric electrolytes based on poly(vinylidene fluoride) and poly(methyl methacrylate) grafted natural

rubber for applications in electrochemical devices. J Solid State Electrochem 2016;20(1):203–13.
[54] Pratap R, Singh B, Chandra S. Polymeric rechargeable solid-state proton battery. J Power Sources 2006;161:702–6.
[55] Woo HJ, Liew C, Majid SR, Arof AK. Poly(ε-caprolactone)-based polymer electrolyte for electrical double-layer capacitors. High Perform Polym 2014;26:637–40, http://dx.doi.org/10.1177/0954008314542168.
[56] Pandey GP, Kumar Y, Hashmi SA. Ionic liquid incorporated PEO based polymer electrolyte for electrical double layer capacitors: a comparative study with lithium and magnesium systems. Solid State Ion 2011;190:93–8, http://dx.doi.org/10.1016/j.ssi.2011.03.018.
[57] Liew CW, Ramesh S. Electrical, structural, thermal and electrochemical properties of corn starch-based biopolymer electrolytes. Carbohydr Polym 2015;124:222–8.
[58] Hashmi SA, Latham RJ, Linford RG, Schlindwein WS. Polymer electrolyte based solid state redox supercapacitors with poly(3-methyl thiophene) and polypyrrole conducting polymer electrodes. Ionics 1997;3:177–83.
[59] Winie T, Jamal A, Saaid FI, Tseng T. Hexanoyl chitosan/ENR25 blend polymer electrolyte system for electrical double layer capacitor. Polym Adv Technol 2018;30:726–35, http://dx.doi.org/10.1002/pat.4510.
[60] Kadir MFZ, Arof AK. Application of PVA–chitosan blend polymer electrolyte membrane in electrical double layer capacitor. Mater Res Innov 2013;15:217–20, http://dx.doi.org/10.1179/143307511X13031890749299.
[61] Pandey GP, Hashmi SA, Kumar Y. Multiwalled carbon nanotube electrodes for electrical double layer capacitors with ionic liquid based gel polymer electrolytes. J Electrochem Soc 2010;157(1):A105–14.
[62] Tiruye GA, Munoz-Torrero D, Palma J, Anderson M, Marcilla R. Performance of solid state supercapacitors based on polymer electrolytes containing different ionic liquids. J Power Sources 2016;326:560–8.
[63] Teoh KH, Lim Chin-Shen, Liew Chiam-Wen, Ramesh S, Ramesh S. Electric double-layer capacitors with corn starch-based biopolymer electrolytes incorporating silica as filler. Ionics 2015;21:2061–8.
[64] Nasibi M, Golozar MA, Rashed G. Nano zirconium oxide/carbon black as a new electrode material for electrochemical double layer capacitors. J Power Sources 2012;206:108.
[65] Liew C, Ramesh S, Arof AK. Enhanced capacitance of EDLCs (electrical double layer capacitors) based on ionic liquid-added polymer electrolytes. Energy 2016;109:546–56, http://dx.doi.org/10.1016/j.energy.2016.05.019.
[66] Shuhaimi NEA, Majid SR, Arof AK. On complexation between methyl cellulose and ammonium nitrate. Mater Res Innovat 2009;13:239–42.
[67] Hashmi SA, Latham RJ, Linford RG, Schlindwein WS. Studies on all solid state electric double layer capacitors using proton and lithium ion conducting polymer electrolytes. J Chem Soc Faraday Trans 1997;93(23):4177–82.
[68] Gu HB, Kim JU, Song HW, Park GC, Park BK. Electrochemical properties of carbon composite electrode with polymerelectrolyte for electric double-layer capacitor. Electrochim Acta 2000;45:1533–6.
[69] Aziz Shujahadeen B, Brza MA, Mishra Kuldeep, Hamsan MH, Karim Wrya O, Abdullah Ranjdar M, et al. Fabrication of high performance energy storage EDLC device from proton conducting methylcellulose: dextran polymer blend electrolytes. J Mater Res Technol 2019, http://dx.doi.org/10.1016/j.jmrt.2019.11.042, xxx(xx):xxx–xxx.
[70] Hamsan MH, Aziz SB, Azha MAS, Azli AA, Shukur MF, Yusof YM, et al. Solid-state double layer capacitors and protonic cell fabricated with dextran from *Leuconostoc mesenteroides* based green polymer electrolyte. Mater Chem Phys 2020;241:122290, http://dx.doi.org/10.1016/j.matchemphys.2019.122290.
[71] Arof AK, Kufian MZ, Syukur MF, Aziz MF, Abdelrahman AE, Majid SR. Electrical double layer capacitor using poly(methyl methacrylate)–C_4BO_8Li gel polymer electrolyte and carbonaceous material from shells of mata kucing (*Dimocarpus longan*) fruit. Electrochim Acta 2012;74:39–45.
[72] Kumar MS, Bhat DK. Polyvinyl alcohol-polystyrene sulphonic acid blend electrolyte for supercapacitor application. Phys B 2009;404:1143–7.
[73] Hamsan MH, Shukur MF, Aziz Shujahadeen B, Yusof YM, Kadir MFZ. Influence of Br as an ionic source on the structural/electrical properties of dextran-based biopolymer electrolytes and EDLC application. Bull Mater Sci 2020;43:30, http://dx.doi.org/10.1007/s12034-019-2008-9.
[74] Aziz Shujahadeen B, Abdulwahid Rebar T, Hamsan Muhamad H, Brza Mohamad A, Abdullah Ranjdar M, Kadir Mohd FZ, et al. Structural, impedance, and EDLC characteristics of proton conducting chitosan-based polymer blend electrolytes with high electrochemical stability. Molecules 2019;24(19):3508, http://dx.doi.org/10.3390/molecules24193508.
[75] Shukur MF. Characterization of ion conducting solid biopolymer electrolytes based on starch-chitosan blend and application in electrochemical devices. Dissertation. Malaysia: University of Malaya; 2015.
[76] Wei YZ, Fang B, Iwasa S, Kumagai M. A novel electrode material for electric double-layer capacitors. J Power Source 2005;141:386–91.
[77] Liew Chiam-Wen, Ramesh S, Arof AK. Investigation of ionic liquid-doped ion conducting polymer electrolytes for carbon-based electric double layer capacitors (EDLCs). Mater Des 2016;92:829–35 (n.d.).
[78] Siyahjani S, Oner S, Singh PK, Varlikli C. Highly efficient supercapacitor using single-walled carbon nanotube electrodes and ionic liquid incorporated solid gel electrolyte. High Perform. Polym 2018;30:971–7, http://dx.doi.org/10.1177/0954008318772333.
[79] Zheng C, Yoshio M, Qi L, Wang HY. A 4 V-electrochemical capacitor using electrode and electrolyte materials free of metals. J Power Sources 2014;260:19–26.
[80] Zhong C, Yida D, Hu W, Zhang J. A review of electrolyte materials and compositions for electrochemical supercapacitors. Chem Soc Rev 2015;44(21):7431–920.